Turkish Journal of Electrical Engineering and Computer Sciences

Volume 15 | Number 3 Article 4

1-1-2007

A Sensitive ANN Based Differential Relay for Transformer Protection with Security against CT Saturation and Tap Changer Operation

HASSAN KHORASHADI ZADEH

ZUYI LI

Turk J Elec Engin, VOL.15, NO.3 2007, © TÜBİTAK

A Sensitive ANN Based Differential Relay for Transformer Protection with Security against CT Saturation and Tap Changer Operation

Hassan KHORASHADI-ZADEH, Zuyi LI
Department of Electrical and Computer Engineering, Illinois Institute of Technology
3301 South Dearborn Street, Chicago, Illinois 60616 USA
e-mail: hkhorash@iit.edu • lizu@iit.edu

Abstract

This paper presents an artificial neural network (ANN) based scheme for fault identification in power transformer protection. The proposed scheme is featured by the application of ANN to identifying system patterns, the unique choice of harmonics of positive sequence differential currents as ANN inputs, the effective handling of current transformer (CT) saturation with an ANN based approach, and the consideration of tap changer position for correcting secondary CT current. Performance of the proposed scheme is studied for a wide variety of operating conditions using data generated from simulation. The results indicate that the proposed scheme provides a fast and sensitive approach for identifying internal faults and is secure against CT saturation and transformer tap changer operation.

Key Words: *Differential protection, power transformer, current transformer saturation, artificial neural network.*

1. Introduction

One of the most important pieces of equipment in power systems is the power transformer, which is used in different sizes, types, and connections. A power transformer functions as a node to connect 2 different voltage levels. Therefore, the continuity of its operation is of vital importance in maintaining the reliability of power supply. Any unscheduled repair work, especially replacement of a faulty transformer, is very expensive and time consuming [1].

According to many years of experience, differential protection provides the best overall protection for a power transformer. In principle, this protection scheme makes use of current difference flowing through different terminals of the transformer so as to distinguish between internal and external faults. It is also well recognized that differential current relays are affected by various factors such as inrush current, over-excitation, transformer tap changer operation, and current transformer (CT) saturation. For example, CT saturation leads to inaccurate current measurement and, therefore, may cause mal-operation of differential relays [2].

In addition, when the transformer tap changer is moved up and down with respect to the middle point at which the relay is adjusted to, the differential relay might initiate a trip signal without the presence of any

fault. This mal-operation is caused by a spill current due to the impact of On Load Tap Changer (OLTC). Normally, the control range of an OLTC might be around 9% of the rated voltage and so the contribution of spill current can also be around 9% [3]. In order to preserve security and avoid unwanted operations of the differential protection, minimum sensitivity level of the relay is increased and is usually set above 20% of the rated current [4]. This leads to poor sensitivity of the differential protection and in most cases it is not possible to detect inter-turn faults in transformer windings. Some phase to ground faults (with fault resistances) at the lower part of the windings might not be detected or not fast enough.

Various methods based on the processing of differential current harmonics have been proposed to detect internal faults of power transformers [5-7]. Ref. [8] discusses 2 categories of those methods, i.e. harmonic restraint (HR) and harmonic blocking (HB) methods. The performance of these methods is considerably affected by the selection of coefficients used in the fault detection relationships, which are usually done by experiments.

To enhance the reliability of differential protection, signals other than current have also been utilized. Ref. [9] proposes the use of voltage signals. In [10], a method based on differential power has been proposed to recognize fault conditions from inrush current conditions. The method proposed in [7] is based on modal transform of voltage and current waveforms. The disadvantages of these methods include the need to use voltage transformers and increased calculation cost for the protection algorithm. Another class of methods identifies fault conditions based on the distortion characteristic of differential current waveforms. The method in [11] operates via measurement of intervals between 2 successive peaks of differential current waveforms. The method in [12] operates based on the duration in which differential current waveform remains near zero [12]. Delayed fault detection is the disadvantage of this group of algorithms. There are still other techniques such as artificial neural networks and fuzzy logic that apply current classification to transformer protection [13,14].

Protective relaying is just as much a candidate for the application of pattern recognition techniques. The majority of power system protection techniques are involved in defining the system state through identifying the pattern of the associated voltage and current waveforms measured at the relay location. This means that the development of adaptive protection can be essentially treated as a problem of pattern recognition/classification, in which artificial intelligence (AI) based algorithms including neural networks are powerful. AI based algorithms possess excellent features such as generalization capability, noise immunity, robustness, and fault tolerance. Consequently, in most cases the decision made by an AI based relay would not be seriously affected by variations in system parameters. AI based techniques have been used in power system protection and encouraging results are obtained [15]. In particular, artificial neural networks (ANNs) have been applied to protective relaying to improve power transformer protection [16-19]. However, most of these approaches do not consider the errors associated with OLTC and might mal-operate in the cases in which current transformers get saturated.

This paper focuses on the application of ANN to differential protection of 3-phase power transformers. In the proposed scheme, different transient states are considered as different patterns, which are recognized by an ANN based algorithm. Positive sequences of differential currents are considered as inputs to ANN. The application of ANN and the unique way of choosing ANN inputs make the proposed scheme more secure against specific non-fault phenomena related to 3-phase power transformers and can provide a better detection of internal faults. Consequently, the proposed scheme improves the performance of transformer differential relay in comparison to traditional approaches. This paper will demonstrate the high sensitivity of the proposed ANN scheme against winding and terminal internal faults and the high stability for exter-

nal faults, inrush currents, over-excitation, and especially tap changer operation and current transformer saturation.

The rest of the paper is organized as follows. The structure of the proposed differential relay is discussed in Section II. Tests in Section III illustrate the performance of the proposed scheme. Section IV concludes this paper.

2. The Structure of the Proposed Differential Relay

A block diagram of the proposed differential relay is shown in Figure 1, where current samples obtained from the relay locations are first pre-processed and then fed into ANN based differential relay for determining whether to generate trip signals.

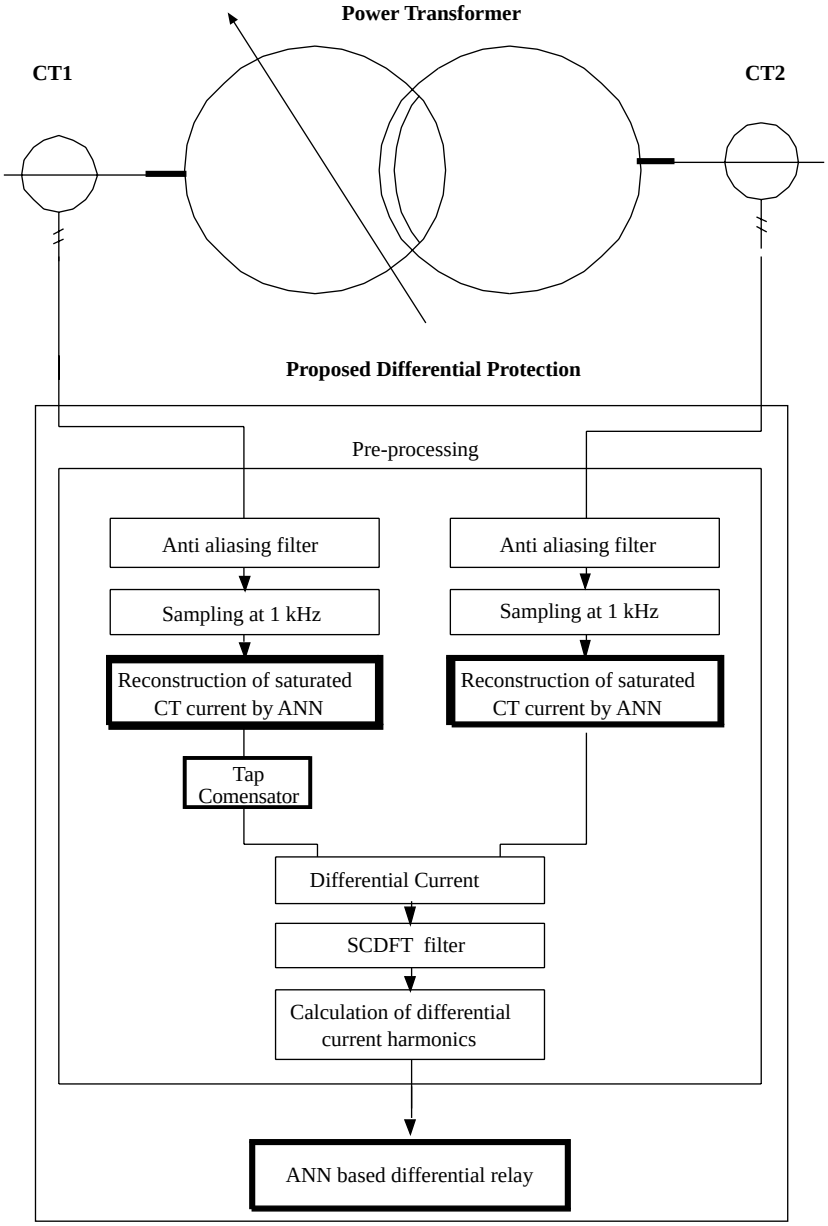

Figure 1. Block diagram of the proposed differential relay.

2.1. Preprocessing

Current samples are first processed by 2nd order low pass anti-aliasing filters, which have a cut-off frequency of 450 Hz, and then sampled at the rate of 1 kHz. Another module is used for reconstructing the secondary CT currents when CT saturation occurs. Differential currents are then calculated accordingly. For more accurate calculation of differential currents, position of the tap changer, which can be obtained using the output signal of the transformer's Automatic Voltage Regulator (AVR), has to be taken into consideration.

The differential current can be calculated using Eq. (1),

$$i_d = i_1(1 \pm Tap) - i_2 \tag{1}$$

where i_d is differential current, i_1 and i_2 are primary and secondary currents of the power transformer, respectively, and *Tap* is the tap position of the transformer.

The magnitudes of certain current harmonics are obtained by symmetrical component discrete Fourier transform (SCDFT) filter from the current samples [2] as follows

$$\begin{cases} I_{dc}(n)_+^{k+1} = I_{dc_+}^k + \Delta i_{da}\cos(nk\theta) + \Delta i_{db}\cos(nk\theta + \dfrac{2\pi}{3}) + \Delta i_{dc}\cos(nk\theta - \dfrac{2\pi}{3}) \\ I_{ds}(n)_+^{k+1} = I_{ds_+}^k + \Delta i_{da}\sin(nk\theta) + \Delta i_{db}\sin(nk\theta + \dfrac{2\pi}{3}) + \Delta i_{dc}\sin(nk\theta - \dfrac{2\pi}{3}) \end{cases} \tag{2}$$

where

$$\theta = \frac{2\pi}{N}$$

$$\Delta i_{da,b,c} = i_{da,b,c}(n) - i_{da,b,c}(n - N + 1) \tag{3}$$

n is the index for current sample.

k is the index for harmonics (1, 2, 5 for the first, second, and fifth harmonic components).

N is the number of samples per cycle (20 in this paper).

$I_{ds}(n)_+, I_{dc}(n)_+$ are the sine and cosine components of the n^{th} harmonics of positive sequence of differential current.

The positive-sequence differential current can be obtained as follows

$$\begin{aligned} I_d(n)_+ &= \sqrt{I_{dc}(n)_+^2 + I_{ds}(n)_+^2} \\ \theta_+ &= Arc\tan(\frac{I_{ds}(n)}{I_{dc}(n)}) \end{aligned} \tag{4}$$

where $I_d(n)_+, \theta_+$ are the magnitude and angle of the positive-sequence differential current.

In the proposed differential relay, the first, second, and fifth harmonic components of the positive sequence differential currents are calculated as inputs to the ANN.

2.2. Reconstruction of CT Current Using ANN

CT saturation and the distortion of CT's secondary current might arise when large short circuit currents occur in the system. CT saturation becomes worse when remnant flux is present in the CT core or when

fault currents include a large amount of decay dc signal. This section highlights the design of an ANN based approach to correct CT saturation caused by faults in power systems [20]. The key idea is that the ANN can learn the inverse function of the CT through training for different power system conditions under which CT saturation occurs. Thus, the primary current of the CT can be accurately estimated once the output from the CT (i.e. the secondary current) is known.

The neural network in [20] is a feedforward network with 30 inputs, 1 output, and 2 hidden layers as shown in Figure 2. The numbers of neurons for the hidden layers are determined empirically and chosen to be 12 and 8 neurons, respectively. Tan-sigmoid function is used as the activation function for the hidden layer neurons, and linear function for the output layer neuron.

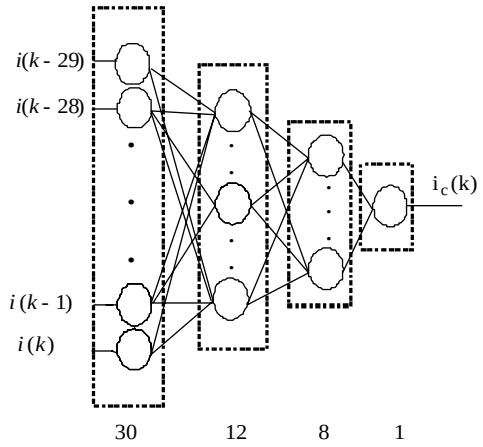

Figure 2. The structure ANN based CT output reconstructing.

A switching algorithm shown in Figure 3 has been used to bypass the network for unsaturated faults [19]. The basic idea is represented by Eq. (5). If the current signal is determined to be saturated, the CT saturation is compensated for by the ANN. Otherwise, the ANN is bypassed and the current signal is used directly as the input to the protection algorithm.

$$\begin{cases} i_{out} = i_{NN}, & \text{if } \left|\dfrac{di_{ct}}{dt} - \dfrac{di_{NN}}{dt}\right| > \varepsilon_1 \text{ and } |i_{ct} - i_{NN}| > \varepsilon_2 \\ i_{out} = i_{ct}, & \text{otherwise} \end{cases} \tag{5}$$

where i_{out}, i_{ct}, and i_{NN} are the outputs of the proposed scheme, the current transformer, and the neural network, respectively. ε_1 and ε_2 are thresholds for detecting CT saturation.

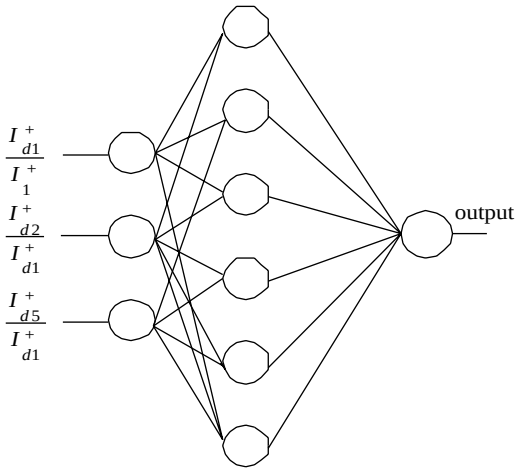

Figure 3. Current selection switching algorithm for reconstruction of the secondary current.

2.3. ANN Based Differential Relay

The proposed differential relay uses multilayer feedforward neural network for detecting internal faults in power transformers. It is well known that the choice of inputs is one of the keys to the success of any ANN application. In [21] it has been shown that the harmonics of the positive sequence of differential current can be used for the detection of different conditions in power transformers. In this paper, the inputs to the ANN based differential unit are I^+_{d1}/I^+_1, I^+_{d2}/I^+_{d1}, and I^+_{d5}/I^+_{d1}, where I^+_{d1}, I^+_{d2}, and I^+_{d5} represent the 1st, 2nd, and 5th harmonic components of the positive sequence differential current, respectively, and I^+_1 represents the positive sequence primary current. The structure of the ANN based differential relay is shown in Figure 4.

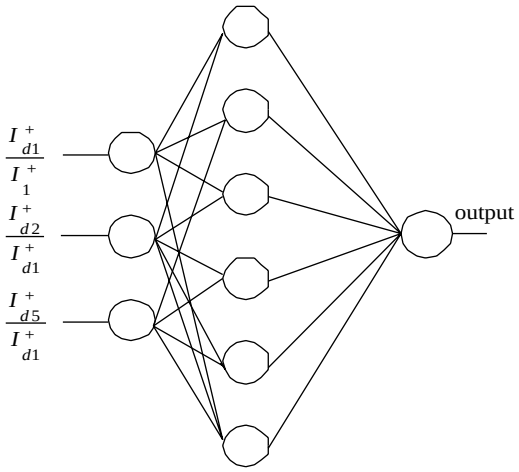

Figure 4. The structure of the ANN based differential relay.

The output layer consists of only 1 neuron with output 1 indicating tripping and output 0 indicating non-tripping. The structure of ANN's hidden layer is determined empirically. One hidden layer with 6 neurons is found to be most appropriate for the differential relay application. A hyperbolic tangent function is used as the activation function of the hidden layer neurons, and saturated linear function for the output layer [22].

Various networks with different number of neurons in their hidden layers were trained with both conventional Back-Propagation (BP) and Marquardt-Levenberg (ML) algorithms [23]. While BP is a steepest descent algorithm, ML algorithm is an approximation to the Newton's method. The ML algorithm is a nonlinear least square algorithm applied to learning of the multilayer perceptrons. The Marquardt-Levnberg update rule is:

$$\Delta W = (J^T J + \mu I)^{-1} J^T e \tag{6}$$

where J is the Jacobian matrix of derivatives of each error to each weight, μ is a scalar, and e is an error vector. If the scalar μ is very large, the above expression approximates gradient descent, while if it is small then it becomes the Gauss-Newton method. It has been found that the neural network trained with the ML algorithm provides better results compared with the neural network trained with the BP algorithm. Therefore, the ML training algorithm is chosen for this application. Convergence is achieved after 25 epochs and the sum square error for training is 0.04 and that for validation phase is 0.085.

3. Test of the Proposed Differential Relay

The proposed ANN based differential relay is trained and tested for various cases such as internal and external faults, inrush current, over-excitation, and different tap positions. Results show that the proposed scheme can detect internal faults under different conditions and can quickly discriminate internal faults from other power system transient states. Some typical results are demonstrated in this section.

3.1. Simulation of the Power System

A 3-phase 230/63 kV power system including a 60 km transmission line, as shown in Figure 5, is used to produce the required training and testing patterns. Table 1 presents some parameters associated with the modeled power system. Simulation studies are performed using the PSCAD/EMTDC software package [24]. The transformer model in [25] is used for simulating the power transformer. The transformer has a delta-star connection and different internal winding faults are simulated.

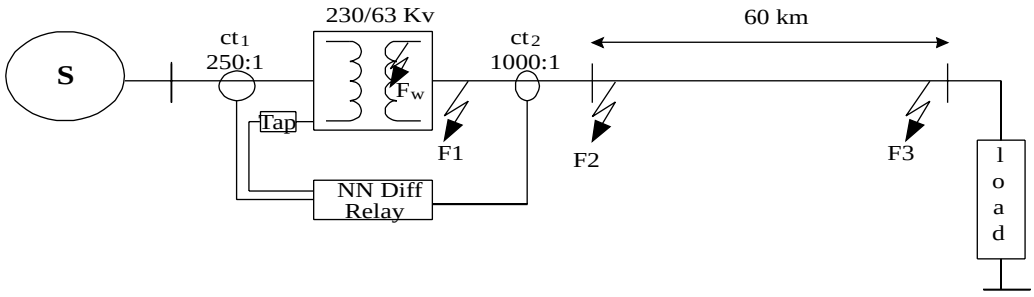

Figure 5. Simulated power system model.

CTs are modeled using the circuit diagram in Figure 6 with their parameters listed in Table 2. The CT ratios are chosen as 1000:1 and 250:1 for secondary and primary of the transformer, respectively. The high accuracy of the CT model has been verified by many tests in [26]. The current transformer is modeled based on the Jiles-Atherton theory of ferromagnetic hysteresis. The effects of saturation, hysteresis, remnance, and minor loop formation are modeled based on the physics of the magnetic material [26].

Table 1. Simulated Power System Parameters.

Transformer reactance (p.u.)	j 0.13
Line impedance, positive and negative sequences (Ω/km)	0.072 + j 0.416
Line impedance, zero sequence (Ω/km)	0.346 + j 1.066

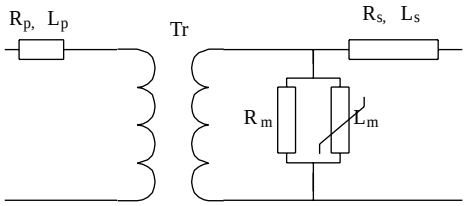

Figure 6. Current transformer circuit diagram.

Table 2. Simulated Current Transformer Parameters.

Secondary winding resistance and leakage inductance (Ω)	0.225, 3.6×10^{-4}	0.5, 8×10^{-4}
Turn ratio	250:1	1000:1
Area (m^2)	6.5×10^{-4}	3.4×10^{-4}
Path length (m)	1.2	0.34
Frequency (Hz)	50	50
Rated voltage (kV)	230	63

3.2. Reconstruction of CT Current

As shown in Table 3, different types of faults on the power system are simulated to generate training patterns for CT current reconstruction. Fault current magnitude, flux remnant, burden, time constant, and fault inception angle are also varied.

Table 3. CT Saturation Training Patterns.

Remnant flux	(-85%)-(85%)	
Fault current magnitude (kA)	Different values between (1-40)	
Burden	Impedance (Ω)	0.5-2
	Power factor	0.5-1
Primary X/R ratio	Different values between (3-63)	
Fault inception angle (°)	Different values between (0-360)	

The training data sets are generated using EMTDC software and then converted to a format usable by MATLAB training algorithms. The ANN training continues until the error reaches an acceptable level. The ANN is then tested with patterns that are not used in training. Test results for 2 different cases are shown in Figures 5 and 6, including the CT primary and secondary currents as well as the current reconstructed by ANN. The output is shown for the first 250 ms after the fault inception, which is of utmost interest.

Figure 7 shows the ANN output for a fault without any flux remnant. The fault inception angle is 180°, the burden resistance is 0.5 Ω, and the X/R ratio is 16. As shown in Figure 7, the proposed ANN is able to estimate primary current correctly.

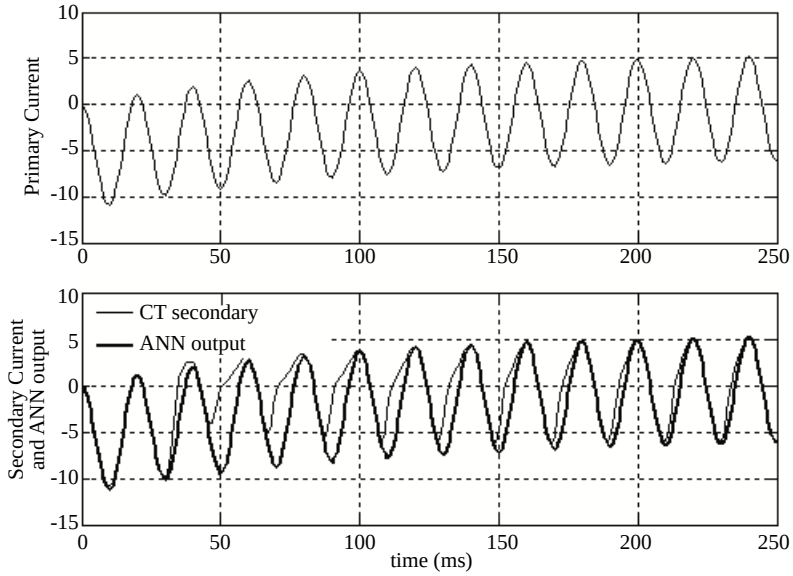

Figure 7. CT primary and secondary currents and ANN output for a fault with $\lambda r = 0$, $\phi = 180$, Rb = 0.5 (Burden), and X/R = 16.

The ANN output for a different fault under a different condition is shown in Figure 8. In this case, fault inception angle is 45°, burden impedance is 0.5 + j0.2 Ω, time constant is 100 ms, and flux remnant is 45%. For this case, the proposed ANN is also able to estimate primary current.

From the above results, as well as many other test cases not reported due to space limitation, it can be observed that the proposed approach successfully estimates the true primary current from a distorted secondary current caused by the CT saturation.

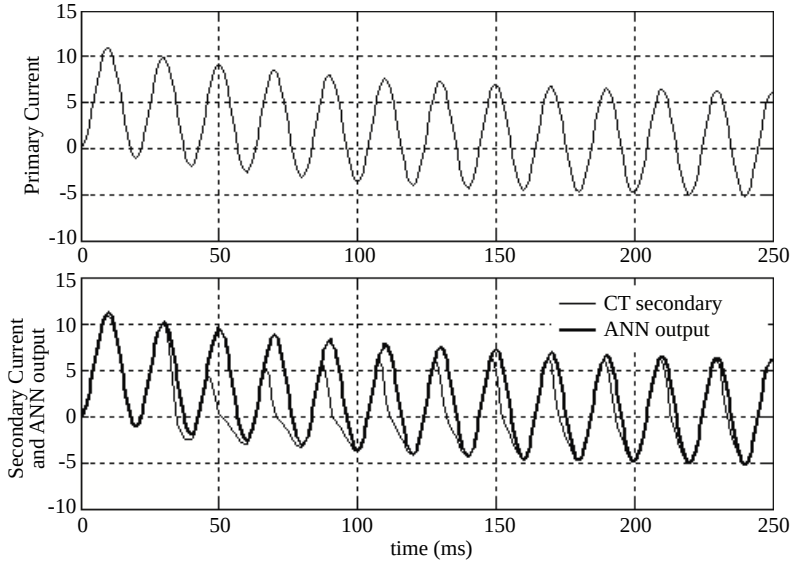

Figure 8. CT primary and secondary currents and ANN output for a fault with $\lambda r = 45\%$, $\phi = 45$, Zb = 0.5 + j0.2 (Burden), and X/R = 32.

3.3. Test Results of the Proposed Differential Relay

The proposed differential relay is trained first with a training data set. Fault type, fault location, source impedance, remnant flux, fault inception time, and other parameters are changed to obtain training patterns covering a wide range of different power system conditions. As shown in Table 4, all types of faults such as phase to ground and phase to phase to ground are considered. These faults occur at different locations, i.e. F1, F2, and F3. Internal winding faults inside the transformer, Fw, are modeled. In addition, various inrush current and over-excitation conditions with different tap settings from –9% to +9% and different amount of loads are considered. The effect of CT saturation is also modeled.

Table 4. System Training Patterns Generation.

System conditions		Fault: AG, BG, ABC, ... at points F1, F2 and F3 Inrush: At different voltage angles Over-excitation: Different amounts of over voltage
Internal winding faults	Turn to turn fault	At different percentage of winding
	Turn to ground fault	At different percentage of winding
Voltage angle (°)		0, 30, 60, and 90
Load (MW)		20, 40, and 100
Remnant flux in transformer core		(-80%) – (80%)
Source impedance (Ω)		12 - 42
Remnant flux in CT core		(-80%) – (80%)
Power angle (°)		(-10) – (10)
Transformer tap setting		(-9%) – (+9%)

A data set consisting of 100 different fault types is generated using the power system model shown in Figure 4. The testing patterns are different from those used to train the network. Fault type, fault inception time, and transformer tap are changed to investigate the effects of these factors on the performance of the proposed scheme.

To compare the performance of the proposed relay with that of the conventional relay, a conventional differential relay has been simulated as shown in Figure 9. The 3-phase relays include 3 single-phase differential relays 1 for each phase. Each single-phase relay also contains a pre-processing module, a differential element, an inrush detector, and an over-flux blocking module. The pre-processing module includes 2nd-order low-pass Butterworth filters as anti-aliasing filters and DFT algorithm to obtain different harmonics of currents. The differential element is a biased differential module and has characteristics as shown in Figure 9. The threshold k_o should be selected based on the magnitude of the magnetizing current and the differential current resulting from the on-load tap-changing during normal loading conditions of the transformer. The slope k_1 of the characteristic should be adjusted to make the differential relay insensitive to transformer tap changing and ratio errors during through fault conditions. In this application $k_0 = 0.1$ and $k_1 = 0$ .25 have been considered. As shown in Figure 9, the relay also includes a magnetizing inrush element and an over-excitation element. These are used to block the relay and prevent unwanted tripping under these conditions. To avoid the unnecessary trip by magnetizing inrush current, the second harmonic

component of current is used for blocking the relay operation. Over-excitation blocking is also activated by checking whether the fifth harmonic component of current is larger than a pre-specified threshold.

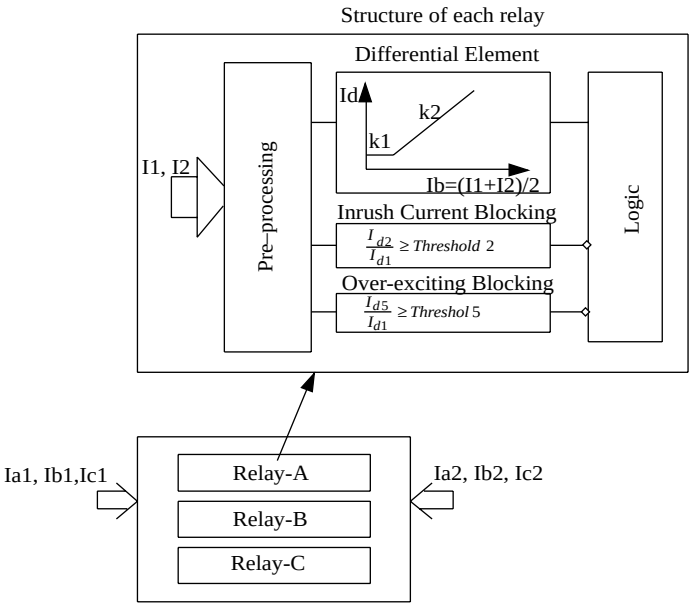

Figure 9. Structure of a 3-phase conventional differential relay.

3.3.1. Relay Response to Internal Faults

The ANN and conventional relay outputs for different kinds of internal faults at F1 are shown in Figure 10. Some of these internal faults are accompanied with inrush current while others do not include simultaneous inrush current. For all the cases, a fault is applied to the system at 25 ms and the relay output is shown for the first 35 ms after the fault inception, which is of utmost interest. As shown in Figure 10, the proposed differential relay and conventional relay are able to respond to the faults correctly, even for the cases in which the current signal includes inrush current. In addition, the ANN based relay operates after an average of about 7 ms, which is quite fast, while the conventional relay operates after at least 16 ms.

Various faults on different phases of the transformer's primary and secondary winding are also generated and used to test the proposed scheme. The results for 2 of these cases are shown in Figures 11 and 12.

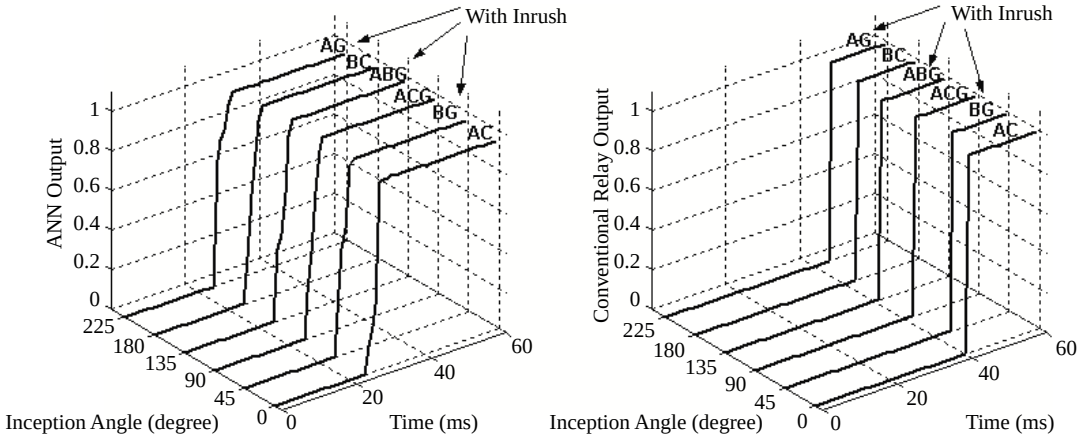

Figure 10. ANN and conventional relay output for different internal faults.

Figure 11 shows the ANN and conventional outputs for a turn to ground fault, which is located at 8.2% from the winding neutral and occurs at 10 ms. We can see that ANN output is activated in just about 5 ms after fault occurrence and then remains stable. This shows that the proposed ANN based differential relay is sensitive enough to detect a ground fault near the neutral end. In comparison, conventional differential relay is not sensitive enough to detect this fault.

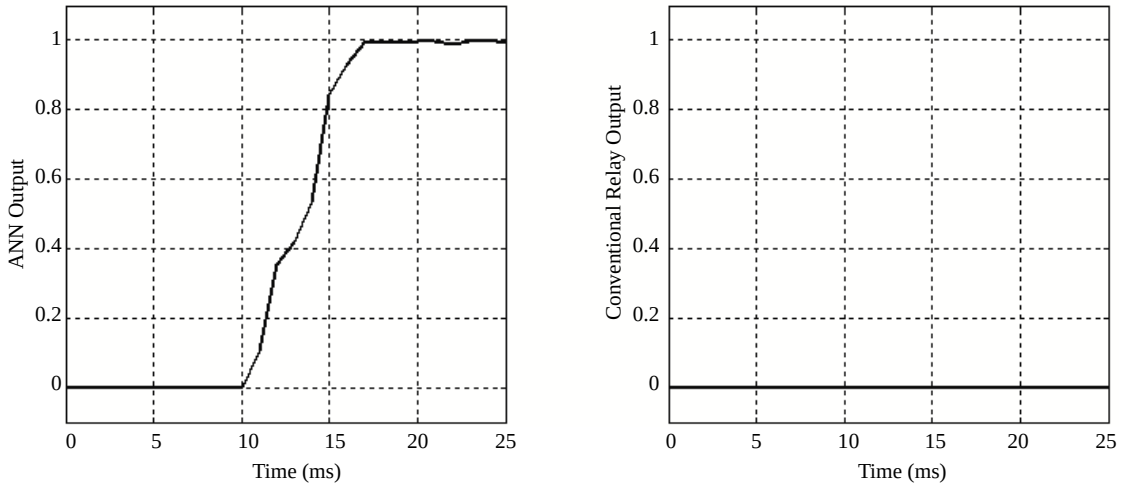

Figure 11. ANN and conventional relay output for an internal turn to ground fault (8.2%).

The relays outputs for an internal turn-to-turn fault are shown in Figure 12. The fault is located between 15% and 20% of the windings. As shown in Figure 12, the ANN relay is able to respond to this internal fault correctly in 5 ms while the conventional relay is not.

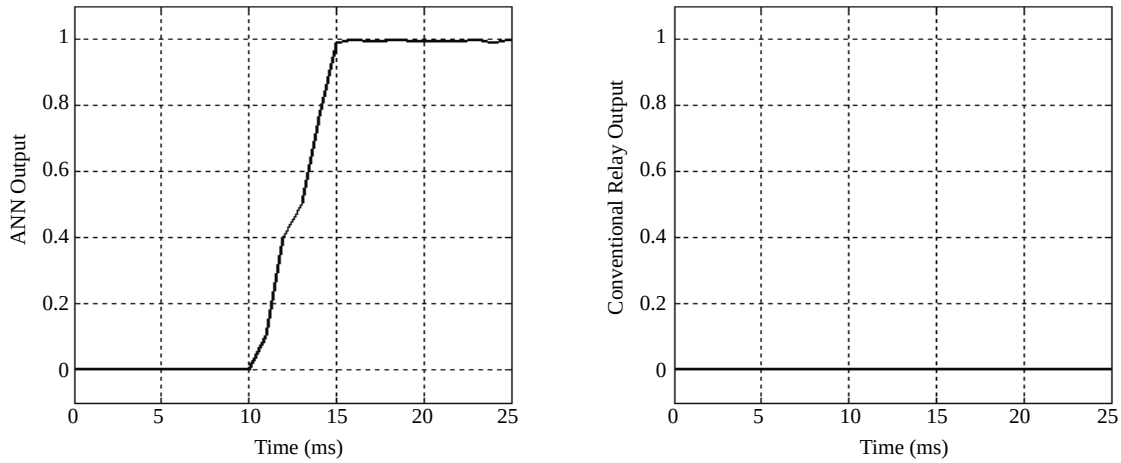

Figure 12. ANN and conventional relay output for an internal turn to turn fault (15%-20%).

3.3.2. Relay Response to Magnetizing Inrush Cases

High inrush currents may be caused by energizing transformers. Although the magnitude of the energization current is only 1%-2% of the transformer rated current under steady state operating conditions, it may become as high as tens of times the rated current when transformers are energized. These transients may cause unnecessary tripping of relays and thus affect the reliability of a power system [4]. ANN and

conventional relay outputs for various inrush conditions with different closing voltage angles are shown in Figure 13. The ANN based relay performs correctly and remains stable as the conventional relay does.

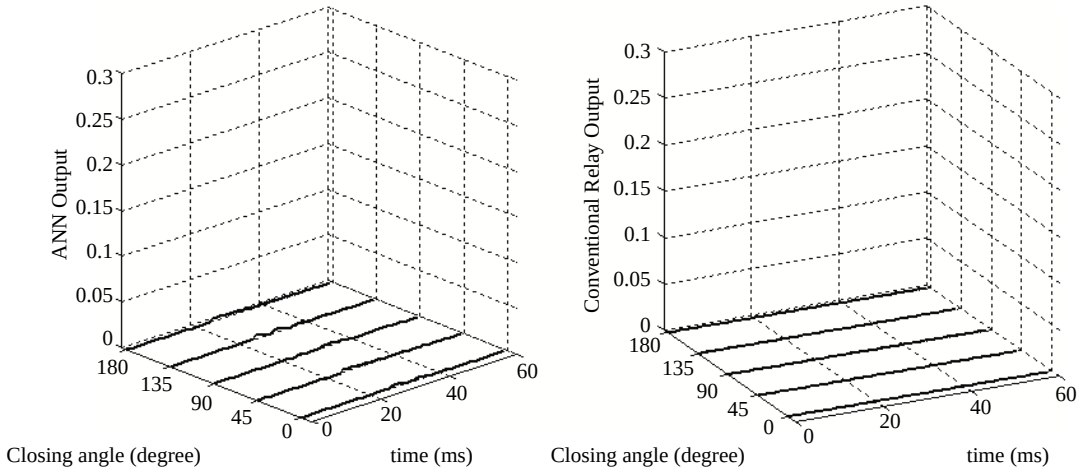

Figure 13. ANN and conventional relay output for different inrush current cases.

3.3.3. Relay Response to Over-excitation

When a large section of the system load is suddenly disconnected from a power transformer, the voltage at the input terminals of the transformer may rise by 10%-20% of the rated value. When the input voltage exceeds the knee point voltage of the power transformer [4], the transformer steady state excitation current may rise significantly, sometimes to a value high enough to activate the differential protection relay, since this current is seen only by the CT on the input side.

Figure 14 shows the ANN and conventional relay outputs for an over-excitation condition as well as the Phase A differential current. We can see that the ANN relay performs correctly and remains stable as the conventional relay does.

3.3.4. Relay Response to External Faults

The responses of the proposed and conventional relays to a few different external faults are tested. Figure 15 shows outputs of the ANN based relay and the conventional relay for an external single phase to ground fault CG at F2 without inrush current. The fault is applied to the system at 10 ms and the transformer tap is at the +9% position. The relay performs correctly and remains stable as the conventional relay does, as shown in Figure 15.

The relay is also tested for a case when the transformer's CTs get saturated. Figure 16 shows CT outputs of phase B for a BG fault at F2. As shown, the secondary CT is saturated. Relay output for this fault with transformer tap at -9% tap is shown in Figure 16. We can see that the relay output remains stable for this fault even though the transformer tap is not at the middle point and the transformer CT is saturated. In comparison, the conventional relay detects this condition as a fault and generates a trip signal.

3.3.5. Additional Performance Studies

The performance of the proposed differential relay for a few different cases with various power system conditions is presented in Table 5. For example, the first row of Table 5 shows that for 1.5% tap the relay

operates correctly for different conditions, including inrush without fault and with closing angle of 20°, internal fault with and without inrush (at F1), and external faults with and without inrush (at F2 and F3).

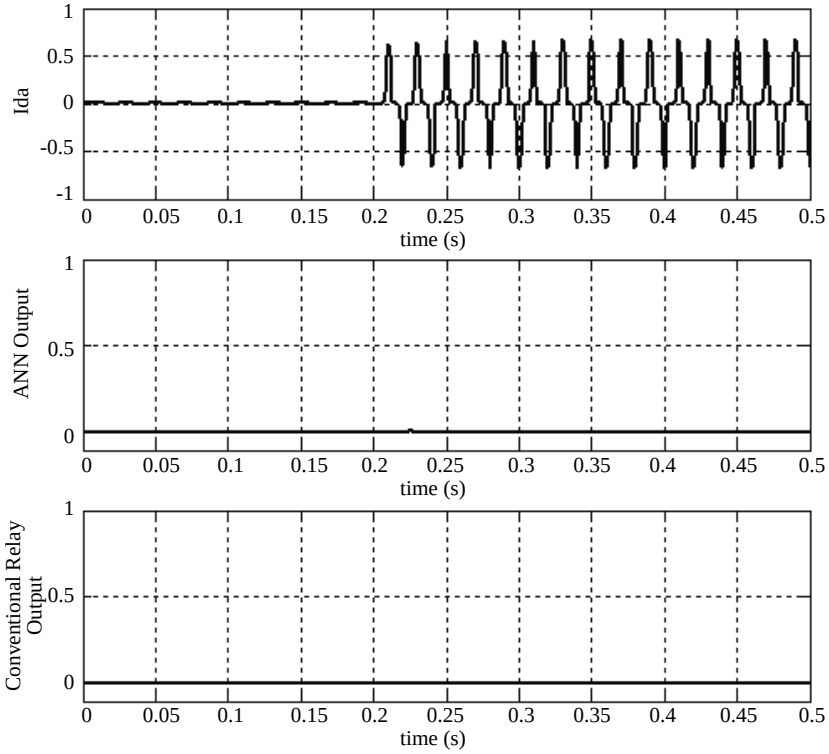

Figure 14. ANN and conventional relay output for an over-excitation case.

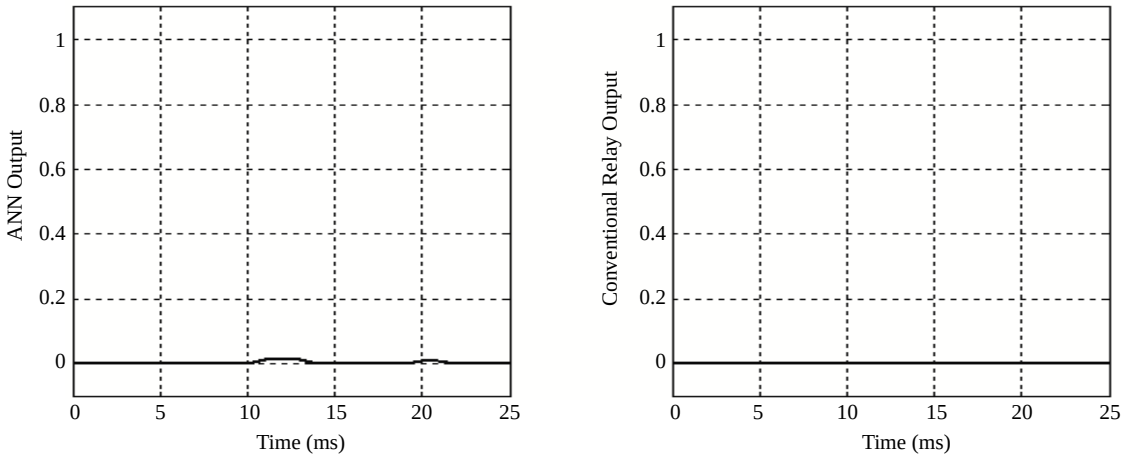

Figure 15. Relay output for external CG fault at F2 without inrush and with 9% tap.

As shown in Table 5, the relay performs very reliably for various cases. The relay responds correctly for various types of faults inside the protection zone, even when the tap is changed or when inrush current exists. Moreover, the relay does not operate for external faults under different conditions.

3.4. Discussion of the Test Results

Performance of the proposed ANN-based scheme has been tested extensively and the following observations can be made.

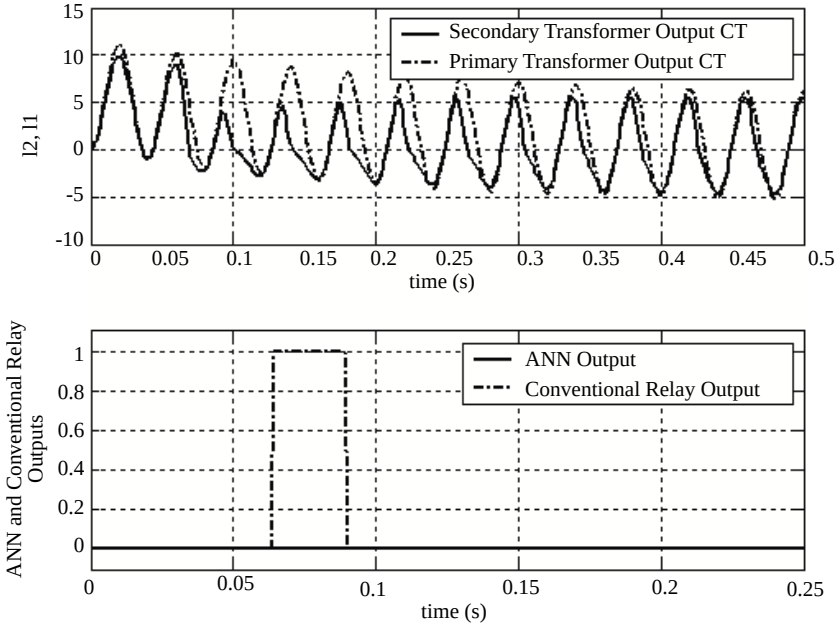

Figure 16. CTs outputs for an external BG fault at F2 and ANN and conventional relay outputs for this fault.

Table 5. Differential Relay Operation Test Results.

Tap	Inrush Without Fault		Fault at F1		Fault at F2		Fault at F3	
3	$\phi^{(1)}$		INR$^{(2)}$	NO-INR $^{(3)}$	INR	NO-INR	INR	NO-INR
1.5	20	No-Trip	F$^{(4)}$: AG Trip	Trip	No-Trip	No-Trip	No-Trip	No-Trip
0	30	No-Trip	F:CG Trip	Trip	No-Trip	No-Trip	No-Trip	No-Trip
3	25	No-Trip	F:AB Trip	Trip	No-Trip	No-Trip	No-Trip	No-Trip
4.5	35	No-Trip	F:AC Trip	Trip	No-Trip	No-Trip	No-Trip	No-Trip
-4.5	25	No-Trip	F:BC Trip	Trip	No-Trip	No-Trip	No-Trip	No-Trip
3	60	No-Trip	F:BG Trip	Trip	No-Trip	No-Trip	No-Trip	No-Trip
4.5	20	No-Trip	F:AB Trip	Trip	No-Trip	No-Trip	No-Trip	No-Trip
-6	45	No-Trip	F:CG Trip	Trip	No-Trip	No-Trip	No-Trip	No-Trip
9	15	No-Trip	F:AC Trip	Trip	No-Trip	No-Trip	No-Trip	No-Trip
4.5	25	No-Trip	F:BG Trip	Trip	No-Trip	No-Trip	No-Trip	No-Trip
-9	20	No-Trip	F:AC Trip	Trip	No-Trip	No-Trip	No-Trip	No-Trip
3	0	No-Trip	F:AB Trip	Trip	No-Trip	No-Trip	No-Trip	No-Trip
1.5	20	No-Trip	F:AC Trip	Trip	No-Trip	No-Trip	No-Trip	No-Trip
-1.5	90	No-Trip	F:BG Trip	Trip	No-Trip	No-Trip	No-Trip	No-Trip
4.5	35	No-Trip	F:AB Trip	Trip	No-Trip	No-Trip	No-Trip	No-Trip
-9	20	No-Trip	F:BG Trip	Trip	No-Trip	No-Trip	No-Trip	No-Trip

$^{(1)}$: Inception angle, $^{(2)}$: Inrush, $^{(3)}$: No-inrush, and $^{(4)}$: Fault

- A wide range of tests has been performed for the proposed scheme and encouraging results are obtained.
- The performance of the proposed scheme has been checked for different transient states, such as magnetizing inrush and over-excitation. The proposed relay operates correctly and remains stable for these cases.
- The proposed scheme has been tested for faults both inside and outside the protected zone and correct responses are obtained.

- For internal faults, the proposed scheme initiates a tripping command at 4-8 ms after fault inception. The proposed scheme operates reliably for different turn to turn and turn to ground faults.
- For external faults, the proposed relay remains stable, even for cases where the tap changes or CTs are saturated.

The advantages of the proposed differential relay over the previous approaches are due to the elimination of OLTC error as well as CT saturation error. Consequently, the sensitivity of the proposed differential relay is increased. Thus the proposed ANN based relay is more dependable to detect lower levels of spill currents. Moreover, as the proposed scheme uses second and fifth harmonic components as its inputs, it provides a secure mechanism against CT saturation and transformer over-excitation problems.

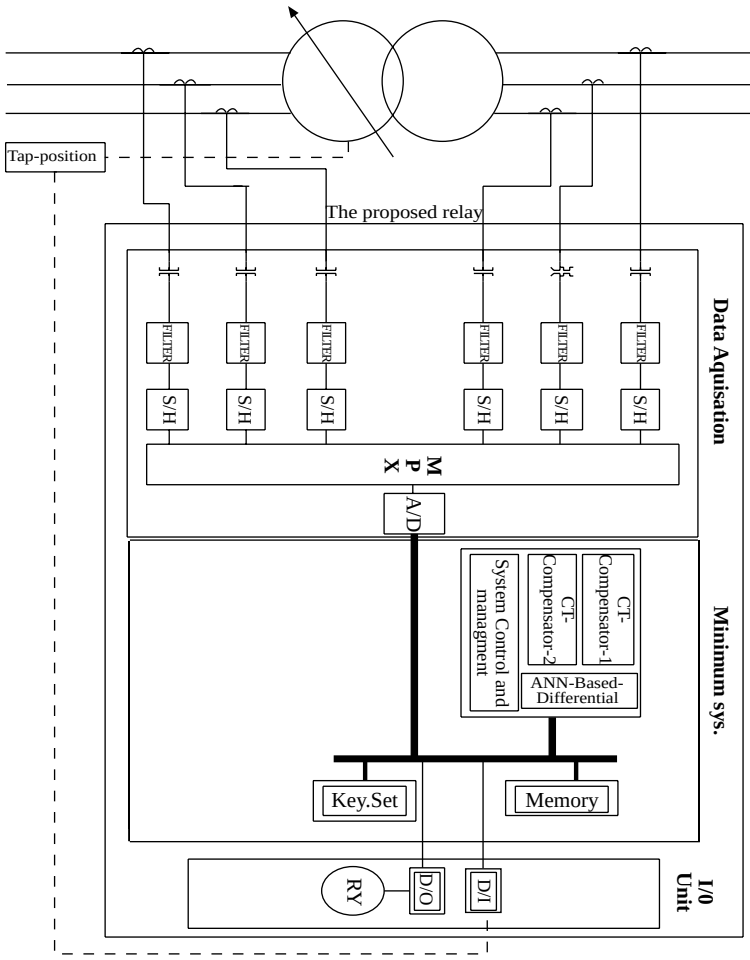

Figure 17. The proposed hardware to implement the proposed scheme.

4. Implementation

The proposed algorithm can be implemented using hardware for a real-world application. The block diagram is shown in Figure 17. The hardware comprises a Data Acquisition System (DAS) card, a minimum system card, and an I/O card. Active low-pass filters, sample holders, an analog multiplexer, and an Analog to Digital (A/D) converter are considered for sampling and analog-to-digital conversion of the instantaneous

current signal. The prepared digitized data are then introduced to the minimum system card. A sampling rate of 20 samples per cycle is assumed in the data acquisition module.

The minimum system card includes a digital signal processor and memory (EPROM & EEPROM). This card controls the data-acquisition process. It also processes the acquired signals and implements the proposed technique. The complete algorithm for 3-phase secondary currents is executed in real time on the digital processor.

The input/output (I/O) card is an interface circuit between digital input/output signals and the measuring logic processor.

5. Conclusion

This paper presents a new scheme based on artificial neural networks differential protection of power transformers. Positive sequence of differential currents are chosen as inputs to ANN. Simulation results show that, with the application of ANN and the unique way of choosing ANN inputs, the proposed differential relay operates properly under different conditions and the diagnosis is both accurate and fast. A compensation technique considering tap position improves the performance of the proposed scheme against tap changer operation. The proposed scheme also uses an ANN to correct CT secondary current under CT saturation condition. Therefore it can operate with proper sensitivity against CT saturation. The proposed scheme has also been implemented on a DSP board to check its performance in real-time operation. Test results will be presented in a future work.

References

[1] A. Phadke, J. Thorp, *Computer Relaying for Power Systems*, Research Studies Press Ltd, Hertfordshire, United Kingdom, 1988.

[2] S. Horowitz, A. Phadke, *Power System Relaying*, 2nd ed. Hertfordshire, United Kingdom, 1995.

[3] R. Israel, R. Jialil, B. Dogra, *Transformers*, Tata McGraw-Hill Publishing Company Limited, New Delhi, 1987.

[4] Electricity Training Association, *Power System Protection, Volume 2, Digital Protection and Signaling*, IEE, London, 1995.

[5] M. Zaman, M. Rahman, "Experimental testing of the artificial neural network based protection of power transformers," IEEE Transactions on Power Delivery, vol. 13, no. 2, pp. 510–517, Apr. 1998.

[6] T. Sidhu, M. Sachdev, H. Wood, M. Nagpal, "Design, implementation, and testing of a microprocessor-based high-speed relay for detecting transformer winding faults," IEEE Transactions on Power Delivery, vol. 7, no. 1, pp. 108–117, Jan. 1992.

[7] T. Sidhu, M. Sachdev, "On-line identification of magnetizing inrush and internal faults in three-phase transformers," IEEE Transactions on Power Delivery, vol. 7, no. 4, pp. 1885–1891, Oct. 1992.

[8] A. Guzman, "Performance analysis of traditional and improved transformer differential protective relays," SEL Technical Papers, pp. 405–412, 2000.

[9] K. Inagaki, M. Higaki, "Digital protection method for power transformers based on an equivalent circuit composed of inverse inductance," IEEE Transactions on Power Delivery, vol. 3, no. 4, pp. 1501–1510, Oct. 1998.

[10] K. Yabe, "Power differential method for discrimination between fault and magnetizing inrush current in transformers," IEEE Transactions on Power Delivery, vol. 12, no. 3, pp. 1109–1117, July 1997.

[11] G. Rockefeller, "Fault protection with a digital computer," IEEE T-PAS-98, pp. 438–464, 1969.

[12] A. Giuliante, G. Clough, "Advances in the design of differential protection for power transformers," Proceedings of the 1991 Georgia Technical Protective Relaying Conference, Atlanta, pp. 1–12, 1991.

[13] O. Youssef, "A wavelet-based technique for discrimination between faults and inrush currents in transformers," IEEE Transactions on Power Delivery, vol. 18, no. 1, pp. 170–176, Jan. 2003.

[14] M. Shin, C. Park, J. Kim, "Fuzzy logic-based relaying for large power transformer protection," IEEE Transactions on Power Delivery, vol. 18, no. 3, pp. 718 – 724, July 2003.

[15] M. Kezunoic, "A survey of neural network application to protective relaying and fault analysis," Eng. International Systems, vol. 5, no. 4, pp.185-192, Dec. 1997.

[16] H. Khorashadi-Zadeh, M. Sanaye-Pasand, "Power transformer differential protection scheme based on wavelet transform and artificial neural network algorithms," Proc. of the 39nd International Universities Power Engineering Conference, pp.747-753, Sept. 2004.

[17] A. Orille-Fernandez, N. Ghonaim, J. Valencia, "A FIRANN as a differential relay for three phase power transformer protection," IEEE Transactions on Power Delivery, vol. 16, no. 2, pp. 215- 218, Apr. 2001.

[18] P. Mao, R. Aggarwal, "A novel approach to the classification of the transient phenomena in power transformers using combined wavelet transform and neural network," IEEE Transactions on Power Delivery, vol. 16, no. 2, pp 654 – 659, Apr. 2001.

[19] J. Pihler, B. Grcar, D. Dolinar, "Improved operation of power transformer protection using artificial neural network," IEEE Transactions on Power Delivery, vol. 12, no. 3, pp. 1128-1135, July 1997.

[20] H. Khorashadi-Zadeh, M. Sanaye-Pasand, "Correction of saturated current transformers secondary current using ANN", IEEE Transactions on Power Delivery, vol. 21, no. 1, pp. 73-79, January 2006.

[21] H. Khorashadi-Zadeh, "Transformer differential protection using positive sequence current; design and implementation," Proc. of the IEEE PowerTech Conference, St. Petersburg, June 2005

[22] S. Haykin, *Neural Networks*, IEEE Press, New York ,1994.

[23] M. Hagan, M. Menhaj, "Training feedforward networks with the marquardt algorithm," IEEE Transactions on Neural Networks, vol. 5, no. 6, pp. 989-993, Nov. 1994.

[24] *PSCAD/EMTDC User's Manual*, Manitoba HVDC Research Center, Winnipeg, Manitoba, Canada, 1988.

[25] B. Kasztenny, M. Kezunovic, Z. Galijasevic, "A new ATP add-on for modeling internal faults in power transformers," American Power Conference, Chicago, Illinois, Apr. 2000.

[26] U. Annakkage, P. McLaren, E. Dirks, R. Jayasinghe, E. Dirks, R. Jayasinghe, "A current transformer model based on the Jiles-Atherton theory of ferromagnetic hysteresis," IEEE Transactions on Power Delivery, vol. 15, no. 1, pp. 57-61, Jan. 2000.